# Transcriptomic and Metabolomic Changes Triggered by Macrosiphum Rosivorum in Rose (Rosa longicuspis)

**Penghua Gao**
Yunnan Academy of Agricultural Sciences
**Hao Zhang**
Yunnan Academy of Agricultural Sciences
**Huijun Yan**
Yunnan Academy of Agricultural Sciences
**Ningning Zhou**
Yunnan Academy of Agricultural Sciences
**Bo Yan**
Southwest Forestry University
**Yuanlan Fan**
Yunnan Academy of Agricultural Sciences
**Kaixue Tang**
Yunnan Academy of Agricultural Sciences
**Xianqin Qiu** ( xianqin711@hotmail.com )
Yunnan Academy of Agricultural Sciences

**Research Article**

**Keywords:** Rose, Rosa longicuspis - Macrosiphum rosivorum interaction, Transcription factors, Starch and sucrose metabolism, Cutin, suberine and wax biosynthesis

**Posted Date:** September 1st, 2021

**DOI:** https://doi.org/10.21203/rs.3.rs-828971/v1



**Version of Record:** A version of this preprint was published at BMC Genomics on December 1st, 2021. See the published version at https://doi.org/10.1186/s12864-021-08198-6.

# Abstract

**Background:** Rose is an important economic horticultural crop. However, its field growth and quality are negatively affected by aphids. However, the defence mechanisms used by rose plants against aphids are unclear. A previous study showed that *Macrosiphum rosivorum* is the most common and harmful aphid species to *Rosa* plants and that *Rosa longicuspis* is highly resistant species to aphids. Therefore, to understand the defence mechanism of rose under aphid stress, we combined RNA sequencing and metabolomics techniques to investigate the changes in gene expression and metabolomic processes in *R. longicuspis* infected with *M. rosivorum.*

**Result:** In our study, after inoculation with *M. rosivorum*, *M. rosivorum* quickly colonized. A total of 34202 genes and 758 metabolites were detected in all samples, with 2845, 2627 and 466 differentially expressed genes (DEGs) were found in CK-vs.-A3 d, CK-vs.-A5 d, and A3 d-vs.-A5 d, respectively. Among these metabolites, 65, 70 and 26 differentially expressed metabolites (DEMs) were found in CK-vs.-A3 d, CK-vs.-A5 d, and A3 d-vs.-A5 d, respectively. The combined omics approach revealed that *M. rosivorum* is perceived by effector-triggered immunity. Under *M. rosivorum* stress, *R. longicuspis* responded by signal transduction pathway activation, transcription factor expression, ROS production and hormone-mediated defence responses. Interestingly, the 'brassinosteroid biosynthesis' pathway was significantly enriched in A3 d-vs.-A5 d. Further analysis showed that *M. rosivorum* induced the transformation of starch and sucrose, the biosynthesis of terpenoids, tannins and phenolic acids and metabolism of cyanoamino acid. Importantly, the 'tropane, piperidine and pyridine alkaloid biosynthesis', 'glutathione metabolic' and 'glucosinolate biosynthesis' pathways were significantly enriched, which resulted in increased levels of metabolites that were involved in the plant defence response.

**Conclusion:** Our study provides candidate genes and metabolites for *Rosa* defence against aphids. What's more, this study provides a theoretical basis for further exploring the molecular regulation mechanism of rose aphid resistance and aphid resistance breeding in the future.


# Background

Rose is one of the most important cut flowers in the world and has high ornamental and economic value [1]. Unfortunately, roses have become prey for many pests due to their high carbohydrate and sugar contents. Among various pests, aphids are the most common predator and affect the yield, quality and ornamental value of rose [2].

Aphids often gather in the immature tissues of roses and damage the immature leaves, shoots, branches and buds of roses by sucking the juice, causing leaf curling, yellowing or abnormal flowering [3, 4]. These aphid species include *Macrosiphum rosae*, *Macrosiphum rosivorum*, *Myzus persicae*, *Myzaphis rosarum* and *Aphis gossypii.* Among them, *Macrosiphum rosivorum* is the most common and serious in rose [5, 6]. At present, insecticides such as pymetrozine and imidacloprid are mainly used to control aphids on rose crops. However, aphids have developed a tolerance to these products due to the long-term use of

chemical drugs. The worse the effect, the larger the drug dosage, which not only increases the economic cost but also aggravates environmental pollution. Therefore, it is urgent to find an ecologically sustainable development method to enhance the resistance of rose to aphids.

With biotechnology developments, whole-genome sequencing of many plant species has been completed, and the results have been applied to study plant growth, environmental interactions and metabolism, among others. In recent years, transcriptomics and metabonomics have been used to explore the defence mechanisms of plant diseases and insect pests, such as rose, maize, and sesame [7–9], thus providing new insights and methods for exploring the mechanism of resistance of rose to aphids.

Aphids are phloem-feeding insects that enter plants through the epidermis and mesophyll using stylet-like mouthparts [10]. During aphid feeding, they secrete saliva containing a series of signals that stimulate the host to generate reactive oxygen species (ROS), thus leading to intracellular oxidative damage [11 ~ 14]. In previous studies, the mechanism of plant defence against aphids can be divided into two types: constructive defence and induced defence. Constitutive defence is a direct defence mechanism, which refers to the defence characteristics of plants that affect aphid feeding behaviour before aphid invasion, such as thorns, wax and trichomes. The accumulation of lignin thickens the cell wall and makes the cambium superlignified, which constitutes a mechanical barrier to insect feeding [15 ~ 17]. Induced defence is a defence characteristic of plants that is activated after aphid attack, and it can be divided into direct defence and indirect defence mechanisms. Induced indirect defences are induced after aphid attack or other stress signals and include the production of volatile substances that attract parasitic and predatory natural enemies for defence; and induced direct defences are a direct defence mechanisms against aphids that directly inhibit the digestion of aphids, such as phytoalexin [18]. Other studies have found that host plants activate their own defence enzyme activities, increase the accumulation of plant endogenous hormones, and promote the synthesis of disease resistance proteins and secondary metabolites to defend against aphids [17, 19, 20].

The germplasm resources of rose in China are rich and have high production and application value; however, they are seriously threatened by aphids. In recent years, research on rose has mainly focused on disease resistance, flower fragrance, continuous flowering, flower colour, etc. [7,21 ~ 23]. The research progress on rose aphids mainly includes three aspects: first, screening and identification of rose aphid-resistant germplasm resources [6]; second, the effect of chemical drugs applied to *Rosa* plants on aphid resistance [24]; and third, the proteomics of aphid resistance in *Rosa* plants [2]. However, few reports on the changes in transcription and metabolites of rose under aphid stress. In this study, *Macrosiphum rosivorum* was inoculated with highly resistant species of *Rosa longicuspis* [6]. The mechanism of resistance of *Rosa* to aphids was explored by transcriptional and metabolic sequencing. These data provide significant information for future rose breeding for resistance to aphids.

# Material And Methods

# Plant growth and plant infection

*R. longicuspis* samples were obtained from the rose germplasm garden of the Flower Research Institute, Yunnan Agriculture Academic Science, Kunming, China.

*M. rosivorum* was applied with a brush to the stem end or undeveloped young leaves of the identified plants, and then the plants were covered with a cylinder, and the plant and aphid grew and reproduced normally [47]. Infected and control plants were individually sampled in a randomized manner from each of the three trays at 3 d and 5 d with three biological repeats for both infected and control treatments at each time point. Leaves were immediately frozen in liquid nitrogen at the time of harvesting and stored at − 80°C.

**Observations of the number of** M. rosivorum

The number of *M. rosivorum* individuals after inoculation for 1 d, 3 d, 5 d and 7 d were counted.

# RNA extraction, library construction and sequencing

Total RNA was extracted using a TRIzol reagent kit (Invitrogen, Carlsbad, CA, USA) according to the manufacturer's protocol. RNA quality was assessed using an Agilent 2100 Bioanalyzer (Agilent Technologies, Palo Alto, CA, USA) and checked using RNase-free agarose gel electrophoresis. After total RNA was extracted, eukaryotic mRNA was enriched by oligo(dT) beads while prokaryotic mRNA was enriched by removing rRNA with a Ribo-Zero™ Magnetic Kit (Epicentre, Madison, WI, USA). Then, the enriched mRNA was fragmented into short fragments using fragmentation buffer and reverse transcribed into cDNA with random primers. Second-strand cDNA was synthesized by DNA polymerase I, RNase H, dNTPs and buffer. Then, the cDNA fragments were purified using a QIAquick PCR extraction kit (Qiagen, Venlo, The Netherlands), end repaired was performed, poly(A) was added, and then the fragments were ligated to Illumina sequencing adapters. The ligation products were size-selected by agarose gel electrophoresis, PCR-amplified, and sequenced using an Illumina HiSeq2500 [48].

# Transcriptomic data analysis

To obtain high-quality clean reads, we removed the adaptor-containing sequences, poly-N, and low-quality reads. The remaining clean reads were further used in the assembly and gene abundance calculation. Then, clean reads were mapped to the reference genome using the HISAT2 tool [49]. For each transcription region, an FPKM (fragment per kilobase of transcript per million mapped reads) value was calculated to quantify its expression abundance and variations using StringTie software [50, 51].

Differential expression analyses among the three treatments (CK-vs.-A3 d, CK-vs.-A5 d, and A3 d-vs.-A5 d with three biological replicates per treatment) were conducted using DESeq2 software [52]. Genes/transcripts with a false discovery rate (FDR) below 0.05 and absolute fold change of ≥ 2 were considered differentially expressed genes/transcripts.

A GO enrichment analysis identified all terms that were significantly enriched in the DEGs compared to the genome background and filtered the DEGs that corresponded to biological functions. KEGG [53] is the major public pathway-related database, and a KEGG pathway enrichment analysis identified significantly enriched metabolic pathways or signal transduction pathways in the DEGs compared with the whole genome background.

# Quantitative real-time PCR validation

qPCR was used to validate the RNA-seq data for 6 different genes. Specific primers were designed using Premier 5 software (Premier Biosoft, Palo Alto, CA, USA). The RNA samples were used to synthesize cDNA, and a Step OnePlus Real-Time Fluorescent Quantitative PCR system (Trans Start® Green qPCR Super Mix) was used to monitor the amount of DNA. Assays of each gene were repeated three times. Quantification was evaluated using the $2^{-(\Delta\Delta Ct)}$ method.

# Extraction and quantification of metabolites

Metabolites were extracted from leaves with three replicates per treatment. The extracted were analysed using an LC-ESI-MS/MS system (UPLC, Shim-pack UFLC SHIMADZU CBM30A, http://www.shimadzu.com.cn/; MS/MS (Applied Biosystems 6500 QTRAP)). LIT and triple quadrupole (QQQ) scans were acquired on a triple quadrupole-linear ion trap mass spectrometer (Q TRAP) [54] and an AB Sciex QTRAP6500 System, equipped with an ESI-Turbo Ion-Spray interface, operating in positive ion mode and controlled by Analyst 1.6.1 software (AB Sciex). The operation parameters were as follows: ESI source temperature 500°C; ion spray voltage (IS) 5500 V; curtain gas (CUR) 25 psi; and collision-activated dissociation (CAD). QQQ scans were acquired as MRM experiments with optimized decluttering potential (DP) and collision energy (CE) for each individual MRM transition [55]. The m/z range was set between 50 and 1000.

Metabolites were identified by searching internal databases and public databases (Mass Bank, KN Ap Sac K, HMDB, Mo to DB, and METLIN) and comparing the m/z values, RT values, and fragmentation patterns with the standards [56].

# Metabolomic data analysis

A T-test was performed, and metabolites with a P value of $< 0.05$ and VIP $\geq 1$ were considered differential metabolites between the groups. We constructed metabolic pathways based on the information in the KEGG database.

# Combined metabolomic and transcriptomic analysis

To reveal the regulatory and influencing mechanism between gene expression and metabolite production, we analysed three models based on gene expression and metabolite abundance. The correlation between the top 250 differentially expressed genes and their metabolites was used to draw a heatmap.

# Results

**Aphid population statistics and leaf morphological changes after inoculation with** M. rosivorum **on** R. longicuspis

To understand the reproduction of aphids, we recorded the number of aphids at 0 d, 1 d, 3 d, 5 d and 7 d. The results showed that the number of aphids increased exponentially and after inoculation for 3 d, 5 d and 7 d, the number of aphids was 2 times, 3.3 times and 3.8 times that of the first inoculation, respectively (Fig. 1). These results indicate that *M. rosivorum* has high reproducibility and ultimately harms the growth conditions of *R. longicuspis.* According to the changes in the aphid population after aphid inoculation, we selected the samples at 0 d, 3 d and 5 d as the research materials and analysed the RNA-seq, qPCR and metabonomics to explore the early mechanism of *Rosa* plants responding to aphid stress.

# Overview of the transcriptomic analysis

To further understand the molecular mechanism underlying the response of *R. longicuspis* to *M. rosivorum*, an RNA-seq analysis was performed. A total of approximately 58.22 GB clean reads were generated from nine biological samples, including six infected and three control samples. The average Q20 value of the raw reads was 95.88% and approximately 84% of the reads were mapped to the reference genome sequences obtained by Trinity splicing. In addition, more than 90.68% of the reads were mapped to the exon region of the reference genome (Table S1). Ultimately, the sequence and expression information of 34202 genes was obtained for subsequent analysis. A principal component analysis (PCA) and Pearson correlation coefficient analysis of the samples based on the FPKM values showed that all the biological replicates exhibited similar expression patterns, indicating the high reliability of our sequencing data (Figure S1). Taken together, the sequencing quality was sufficient for further analysis.

**Identification of DEGs in** R. longicuspis inoculated with M. rosivorum

To obtain a comprehensive view of the gene expression profile associated with the response of *R. longicuspis* to *M. rosivorum*, we used DESeq2 to identify the DEGs. Based on the filtering parameters of FDR < 0.05 and |log2FC|>1, the expression levels of 2845 (1186 upregulated, 1659 downregulated), 2627 (886 upregulated, 1741 downregulated) and 466 (178 upregulated, 288 downregulated) genes were found to differ significantly in the CK-vs.-A3 d, CK-vs.-A5 d, and A3 d-vs.-A5 d groups, respectively. Among those genes, 998 and 904 DEGs were expressed in A3 d and A5 d, respectively (Fig. 2). These results indicate that a large number of genes were upregulated and that few new DEGs were expressed in the *R. longicuspis-M. rosivorum* interaction.

To understand the functions of the DEGs associated with *M. rosivorum*, those DEGs were annotated using GOsEq. This annotation resulted in three major categories: biological processes, cellular components, and molecular functions. A comparison of the CK at 3 d and 5 d indicated that most of the DEGs were enriched in the ‘external encapsulating structure’, ‘cell periphery’, ‘cell wall’, ‘cytoskeleton-dependent cytokinesis’ and ‘histone lysine methylation’ categories and other terms. A comparison of 3 d with 5 d showed that most of the DEGs were enriched in the ‘response to reactive oxygen species’,

‘response to oxidative stress’, ‘response to oxygen-containing compound’ and other terms (Fig. 3A). To better understand the main pathways activated under *M. rosivorum* stress, we conducted a Kyoto Encyclopaedia of Genes and Genomes (KEGG) enrichment analysis of the DEGs. Between the CK and A3 d libraries, 492 DEGs were assigned to 113 KEGG pathways. Between the CK and A5 d libraries, 484 DEGs were assigned to 109 KEGG pathways. Among these pathways, ‘biosynthesis of secondary metabolites’, ‘metabolic pathways’, ‘phenylpropanoid biosynthesis’, ‘fatty acid biosynthesis’, ‘galactose metabolism’, ‘cutin, suberine and wax biosynthesis’, ‘cyanoamino acid metabolism’ and ‘sesquiterpenoid and triterpenoid biosynthesis’ were significantly enriched. Between the A3 d and A5 d libraries, 105 DEGs were assigned to 51 KEGG pathways. Among these pathways, some were related to plant insect resistance pathways associated with the terms ‘plant-pathogen interaction’, ‘starch and sucrose metabolism’, ‘monoterpenoid biosynthesis’ and ‘brassinosteroid biosynthesis’ (Fig. 3B). Taken together, the results showed that under *M. rosivorum* stress, the antioxidant system, terpenoid synthesis and secondary metabolite biosynthesis of *R. longicuspis* were activated to reduce aphid damage in *R. longicuspis*.

Heatmaps of DEG subclusters were developed to better understand the key DEGs associated with the resistance of *R. longicuspis* to *M. rosivorum.* The resulting heatmaps showed the DEGs involved in *R. longicuspis-M. rosivorum* interactions. Based on their functional annotation, these genes included 1 reactive oxygen species metabolic pathway gene, 3 secondary metabolite synthesis genes, and 13 glutathione metabolism genes, which are shown in the heatmap (Fig. 4). These findings indicated that *R. longicuspis* responds to *M. rosivorum* by activating the expression of signal transduction pathway genes, secondary metabolite synthesis genes, antioxidant stress genes and disease resistance genes.

# Validation of candidate DEGs based on qPCR analysis

To validate the reliability of the DEGs obtained from the RNA-Seq analyses, the expression levels of 6 candidate genes were analysed using qPCR. These genes included the 1 α-linolenic acid metabolism gene (*Rl AOC*), 1 starch and sucrose metabolism gene (*Rl BGLU11*), 2 plant-type cell wall modification genes (*Rl EXPB3* and *Rl EXPA1*), 1 hormone response gene (*Rl MBF1C*) and 1 homologous recombination gene. The correlation coefficients (r) between the RNA-Seq and qPCR results were calculated for these DEGs (Figure S2; Table S2). The results showed that the correlation coefficients were greater than 0.75, indicating that the RNA-Seq data were reliable.

# Overview of the metabonomic Analysis

To understand the changes in metabolites and the possible defence mechanisms of *R. longicuspis* to infection by *M. rosivorum*, a metabolite profiling analysis of the *R. longicuspis* leaf samples (CK, A3 d, A5 d) was performed. A total of 758 metabolites were detected in all samples, and they could be divided into 35 groups (Table S3). The principal component analysis (PCA) showed that the repeatability of different treatments was good. Orthogonal partial least squares discriminant analysis (OPLS-DA) showed that the results of OPLS-DA analysis could be used for subsequent model tests and differential metabolite analysis. Between the CK and A3 d treatments, 31 were upregulated and 34 were downregulated. Between the CK and A5 d treatments, 32 were upregulated and 38 were downregulated. The levels of α-linolenic

acid*, γ-linolenic acid*, 2-O-salicyl-6-O-galloyl-D-glucose, scopoletin-7-O-glucuronide, and geniposide increased significantly with the extension of infection time. This finding indicated that these secondary metabolites were involved in the resistance response of *R. longicuspis* to *M. rosivorum.*

To identify the main pathways that *R. longicuspis* uses to respond to *M. rosivorum*, we mapped the differentially expressed metabolites based on a KEGG biological pathway analysis. A total of 283 metabolites were assigned to 94 KEGG pathways, including 'metabolic pathways' (59.72%), 'biosynthesis of secondary metabolites' (36.75%), and 'biosynthesis of antibiotics' (18.73%), among others (Table S4). Sixty-eight significantly differentially expressed metabolites between the CK and A3 d treatments were assigned to 43 KEGG pathways, including 'alpha-linolenic acid metabolism', 'cyanoamino acid metabolism', 'tropane, piperidine and pyridine alkaloid biosynthesis' and others (Table S5). Seventy significantly differentially expressed metabolites between the CK and A5 d treatments were assigned to 43 KEGG pathways, including 'aminoacyl-tRNA biosynthesis', 'cyanoamino acid metabolism', 'glucosinolate biosynthesis' and others (Table S6). Twenty-six significantly differentially expressed metabolites between the A3 d and A5 d treatments were assigned to 15 KEGG pathways, including 'alpha-linolenic acid metabolism' and 'biosynthesis of unsaturated fatty acids' (Table S7). The results showed that the metabolic pathways related to disease resistance were significantly enriched, indicating that the defence mechanism of *R. longicuspis* was activated under *M. rosivorum* stress.

# Glucosinolate biosynthesis

The glucosinolate biosynthesis pathway is involved in plant defence against insects. In our research, 15 metabolites of the glucosinolate biosynthesis pathway exhibited different levels in different treatments (Fig. 5). Among those metabolites, the content levels of L-isoleucine*, L-valine and L-tyrosine were decreased significantly; moreover, compared with the CK, the levels in A3 d and A5 d increased by factors of 1.62, 2.11, and 1.64 and 2.63, 3.06, and 1.64, respectively. In addition, the contents of pyruvic acid, 3-methyl-2-oxobutanoic acid*, (S)-2-hydroxy-2-methyl-3-oxobutanoic acid*, (R)-3-hydroxy-3-methyl-2-oxopentanoic acid* and 2-isopropylmalic acid increased. These results indicate that the glucosinolate biosynthesis pathway may be positively involved in the interaction between *R. longicuspis* and *M. rosivorum.*

# Glutathione metabolism

Glutathione plays an important role in plant resistance to external stress and reactive oxygen species injury. The ratio of reduced glutathione to oxidized glutathione is one of the important indicators of glutathione activity. In our research, the contents of oxiglutatione and NADP (nicotinamide adenine dinucleotide phosphate) decreased continuously (Fig. 5). Compared with the CK, oxiglutatione decreased by 35.15% and 55.29% in A3 d and A5 d, respectively, and NADP decreased by 12.92% and 17.63% in A3 d and A5 d, respectively. The content level of dehydroascorbic acid first increased and then decreased. Compared with the CK, dehydroascorbic acid increased by 12.42% and 3.86% in A3 d and A5 d, respectively, and L-glutamic acid* increased by 12.08% and 10.84% in A3 d and A5 d, respectively. The results showed that *M. rosivorum* infection induced the antioxidant system of *R. longicuspis* and

dehydroascorbic acid and GSH were involved in *R. longicuspis* resistance to oxidative stress caused by *M. rosivorum*..

# Conjoint analysis

A conjoint KEGG enrichment analysis showed 84 comapped pathways, with 35 and 16 comapping pathways between CK-vs.-A3 d and CK-vs.-A5 d and their metabolites, respectively. Interestingly, of these comapped pathways, ‘fatty acid biosynthesis’, ‘metabolic pathways’ and ‘biosynthesis of secondary metabolites’ were significantly enriched in CK-vs.-A3 d, and ‘2-oxocarboxylic acid metabolism’, ‘alpha-linolenic acid metabolism’, ‘sesquiterpenoid and triterpenoid biosynthesis’, ‘linolenic acid metabolism’ and ‘glucosinolate biosynthesis’ were significantly enriched in CK-vs.-A5 d (Fig. 6), indicating that the metabolic pathway related to aphid resistance was activated during aphid stress.

Based on the O2PLS model, the combined analysis of transcriptomics and metabonomic data showed that the model was reliable ($R2 > 0.84$). The Pearson correlation coefficients showed that the differential expression patterns of DEGs and metabolites were consistent. The correlations between the top 250 DEGs and their metabolites were further selected and are represented as a heat map (Figure S3).

## Discussion

# RNA-seq study for disease resistance

Aphids damage the new shoots, young leaves and flower buds of rose plants, which can lead to the decline of rose growth, hinder normal growth or blooming, and seriously affect the ornamental value [6]. To understand the mechanism of rose tolerance to aphids, RNA-Seq and metabolomics were employed to analyse the DEGs and DEMs in *R. longicuspis* at different time points after inoculation with *M. rosivorum.* In our study, DEGs were significantly enriched in ‘fatty acid biosynthesis’, ‘biosynthesis of secondary metabolites’, ‘phenylpropanoid biosynthesis’, ‘starch and sucrose metabolism’, ‘sesquiterpenoid and triterpenoid biosynthesis’, ‘phenylalanine, tyrosine and tryptophan biosynthesis’, ‘cutin, suberine and wax biosynthesis’, ‘alpha-linolenic acid metabolism’ and other pathways related to plant disease and insect resistance. Interestingly, ‘phosphatidylinositol signalling system’ and ‘MAPK signalling pathway - plant’ pathway genes were also activated. All of these transcriptomic data indicated that multiple processes in *R. longicuspis* are associated with plant defence against aphids, which is consistent with the fact that the plants have evolved a complex defence mechanism [25, 26]. Under *M. rosivorum* stress, the expression of a series of antioxidant-, plant hormone- and disease resistance-related genes is induced in *R. longicuspis*, including ROS production genes, GST genes, PTI genes and RPM genes, which were significantly upregulated (Fig. 4). This result revealed that *M. rosivorum* infection induced a change in reactive oxygen species and led to effector-triggered immunity in *R. longicuspis*.

Brassinosteroids (BRs) play an important role in plant growth, developmental processes, and responses to pathogen infection, although the role of BRs in the interactions between plants and insects is still unclear. Liu et al. [27] found that brassinosteroids (BRs) could enhance *Rhagoletis batava obseuriosa*

resistance in sea buckthorn (*Hippophae rhamnoides*). Liao et al. [28] found that BR contributes to the growth-defence tradeoff by suppressing the expression of defensin and glucosinolate biosynthesis genes. Pan et al. [29] demonstrated that BRs promote the susceptibility of rice (*Oryza sativa*) plants to BPH (*Nilaparvata lugens*) by modulating the SA and JA pathways. Interestingly, the expression of genes in the 'brassinosteroid biosynthesis' pathway increased significantly in A3 d vs. A5 d. Therefore, the mechanism of brassinolate on the interaction between rose and aphids is worthy of further study.

As important regulatory factors, transcription factors play an important role in regulating the plant response to environmental signal stimulation. Related transcription factors can be roughly divided into six categories: AP2/ERF family, bHLH family, bZIP family, MYB family, NAC family and WRKY family [30, 31]. Overexpression of *CmWRKY48* in chrysanthemum can improve its defence against aphids [32]. *Arabidopsis MYB102* increases host susceptibility to GPA through ET-dependent signalling pathways [33]. In our study, the expression of 5 transcription factors, namely, 1 bZIP transcription factor (*Rl ABF2*) and 4 MYB transcription factors (*Rl RVE7/8, Rl PHL5 and Rl MYR2*), was significantly higher than that in the control (Figure S4). These results suggest that these five transcription factors may be involved in the response of rose to aphids. Taken together, the results show that under *M. rosivorum* stress, the *R. longicuspis* signal transduction pathway is activated to induce related transcription factors to regulate the expression of downstream disease resistance genes.

# Metabolomics study for disease resistance

Secondary metabolites, such as flavonoids, terpenoids, phenols and alkaloids, have the characteristics of antibiotics and thus play an important role in the defence of phytophagous insects [34, 35]. Terpenoids, flavonoids and tannins enhance plant defence against aphids by affecting aphid colonization [36–39]. Our metabolomics results highlighted differential changes in 15 major classes of metabolites. The contents of eight secondary metabolites, including organic acids, lipids, phenolic acids, lignans and coumarins, terpenoids, tannins, flavonoids, and cis-p-coumaric acid 4-O-glucoside*, increased significantly. Starch sucrose metabolism plays an important role in the defence of phytophagous insects. Previous studies have shown that the accumulation of starch in *Solanum lycopersicum* enhances its defence against peach aphids (*Myzus persicae*) [40]. In our research, the starch synthase SS1 (*Rl SS1*), trehalose 6-phosphate phosphatase (*Rl TPPA*) and β-glucosidase (*Rl BGLU11*) genes were upregulated while the contents of D-glucose 6-phosphate* and glucose-1-phosphate* genes were significantly downregulated, indicating that under aphid stress, rose enhanced its defence against aphids by promoting starch synthesis.

# Aphid Stress Triggered Glucosinolate Accumulation

Glucosinolates can be used as biological insecticides to effectively control aphids [41]. Lei et al. [42] showed that overexpression of the *AtCCA1* gene enhanced resistance to peach aphids by increasing the content of glucosinolates in Arabidopsis (*Arabidopsis thaliana*). Under aphid stress, the expression of related genes and the content of metabolites increased significantly in rose. Thus, the glucosinolate metabolic pathway may be involved in the resistance of *R. longicuspis* to *M. rosivorum.*

# Aphid stress triggers changes in glutathione metabolism

Glutathione plays a crucial role in the defence responses of plants to biotic stress factors [43, 44]. *Rhopalosiphum padi* and *Sitobion avenae* were shown to induce the expression of AsA-GSH cycle-related genes in maize (*Zea mays* L.) and affect the contents of reduced and oxidized ascorbic acid and glutathione [45]. Glutathione metabolic pathway genes were significantly induced and expressed in *Sorghum bicolor* under *Melanaphis sacchari* stress [46]. Our study showed that under aphid stress, the contents of dehydroascorbic acid and L-glutamic acid* were higher than those of the control. However, the contents of oxiglutatione and NADP were lower than that of the control. The expression of glutathione metabolic pathway genes (*Rl ODCs*, *Rl APXs*, *Rl GSTs*, and *Rl HSP26-As*, Fig. 4) was induced. *R. longicuspis* appeared to compensate for the effects of oxidative stress induced by *M. rosivorum* by the elevated expression of genes and affect the content of metabolites involved in the AsA-GSH cycle.

## Conclusion

We combined transcriptome and metabolome analyses to explore the response mechanism of *R. longicuspis* to *M. rosivorum.* Under *M. rosivorum* stress, the signal transduction pathway and defence response of *R. longicuspis* were activated. *M. rosivorum* infection induced a series of signal transduction, MAPK signalling, inositol phosphate signalling, ROS signalling, and endogenous hormone signalling pathways and induced the expression of related genes (*bZIP* and *MYB* transcription factors and *PTI* genes). Interestingly, the ‘brassinosteroid biosynthesis’ pathway was significantly enriched in A3 d-vs.-A5 d. The defence responses included the transformation of starch and sucrose, the synthesis of terpenoids, tannins and phenolic acids and activation of related disease resistance metabolic pathways, namely, ‘biosynthesis of secondary metabolites’, ‘metabolic pathways’, ‘phenylpropanoid biosynthesis’, ‘fatty acid biosynthesis’, ‘cutin, suberine and wax biosynthesis’, ‘cyanoamino acid metabolism’. According to the metabolomic data analysis, glucosinolate metabolism and the glutathione metabolic pathway were significantly enriched. Our study provides candidate genes and metabolites for rose defence against aphids. This study provides a theoretical basis for further exploring the mechanism underlying the molecular regulation of rose aphid resistance and aphid resistance breeding in the future.

## Declarations

### Authors’ contributions

XQQ, KXT and PHG are the experimental designers and executors of this study; HZ, HJY, NNZ, YLF and BY participate in the experimental guidance, and PHG participate in the data processing and paper writing. All authors reviewed the manuscript.

### Acknowledgements

We are thankful to master Yuchun Chen and Yanhong Guo from Academy of Life Sciences, Yunnan University for their assistance with the experiment.

### Funding

This work was supported by funds from the National Key R & D Program of China (No. 2018YFD1000400), the National Natural Science Foundation of China (No. 31860571 and 31560565), the Major Science and Technology Projects Yunnan Province (No. 2016ZA005), youth top-notch talents training project of ‘ten thousand talents plan’ of Yunnan Province and leading talents of Yunling industrial technology

### Availability of data and materials

The Sequence dataset used and/or analyzed during the current study are available from the corresponding author on reasonable request.

### Ethics approval and consent to participate

Not applicable.

### Consent for publication

Not applicable.

### Competing interests

The authors declare that they have no competing interests

### Author details

[1,2] *Flower Research Institute, Yunnan Academy of Agricultural Sciences/ National Engineering Research Center for Ornamental Horticulture, Kunming 650205, China*

[3] *Southwest Forestry University, Kunming 650024, China*

### Publisher’s Note



# References

1. Debener T, Byrne DH. Disease resistance breeding in rose: current status and potential of biotechnological tools. *Plant Science*. 2014, 228:107–117.
2. Muneer S, Jeong HK, Park YG, Jeong, BR. Proteomic analysis of aphid-resistant and sensitive rose (*Rosa Hybrida*) cultivars at two developmental stages. *Proteomes*. 2018, 6(2): 25. doi: 10.3390/proteomes6020025.

3. Mehrparvar M, Mansouri SM, Hatami B. Some bioecological aspects of the rose aphid, *Macrosiphum rosae* (Hemiptera: Aphididae) and its natural enemies. *Acta Universitatis Sapientiae Agriculture & Environment*. 2016, 8(1): 74–88.
4. Fang Y, Qiao GX, Zhang GX. Diversity of host plants and feeding sites of aphids. *Zoological Systematics*. 2006, (01):31–39.
5. Golizadeh A, Jafari BV, Razmjou J, Naseri B, Hassanpour M. Population growth parameters of rose aphid, *Macrosiphum rosae* (Hemiptera: Aphididae) on different rose cultivars. *Neotrop Entomol*. 2017, 46(1): 100–106. doi: 10.1007/s13744-016-0428-4.
6. Fan YL, Chen YC, Jian HY, Yan HJ, Zhang T, Li SF, et al. Screening of aphid resistant germplasm resources of Rosa. *Journal of Yunnan University (Natural Sciences Edition)*. 2021, 43(03): 619–628.
7. Gao PH, Zhang H, Yan HJ, Wang QG, Yan B, Jian HY, et al. *RcTGA1* and glucosinolate biosynthesis pathway involvement in the defence of rose against the necrotrophic fungus *Botrytis cinerea*. *BMC Plant Biol*. 2021, 21(1): 223. doi: 10.1186/s12870-021-02973-z.
8. Wang XJ, Zhang X, Yang JT, Wang ZX. Effect on transcriptome and metabolome of stacked transgenic maize containing insecticidal cry and glyphosate tolerance epsps genes. *The Plant Journal*. 2018, 93(6): 1007–1016. doi: 10.1111/tpj.13825.
9. Zhang Y, Li DH, Zhou R, Wang X, Dossa K, Wang LH, et al. Transcriptome and metabolome analyses of two contrasting sesame genotypes reveal the crucial biological pathways involved in rapid adaptive response to salt stress. *BMC plant biology*. 2019, 19(1): 66. doi: 10.1186/s12870-019-1665-6.
10. Silva SC, Estevez JM, Blanco HF. Influence of cell wall polymers and their modifying enzymes during plant-aphid interactions. *J Exp Bot*. 2020, 71(13): 3854–3864. doi: 10.1093/jxb/erz550.
11. Woźniak A, Bednarski W, Dancewicz K, Gabryś B, Borowiak SB, Bocianowski J, et al. Oxidative stress links response to lead and *Acyrthosiphon pisum* in Pisum sativum L. *J Plant Physiol*. 2019, 240: 152996. doi: 10.1016/j.jplph.2019.152996.
12. Powell G, Tosh CR, Hardie J. Host plant selection by aphids: behavioral, evolutionary, and applied perspectives. *Annu Rev Entomol*. 2006, 51: 309–30. doi: 10.1146/annurev.ento.51.110104.151107.
13. Sytykiewicz H, Łukasik I, Goławska S, Chrzanowski G. Aphid-triggered changes in oxidative damage markers of nucleic scids, proteins, and lipids in maize (*Zea mays* L.) deedlings. *Int J Mol Sci*. 2019, 20(15): 3742. doi: 10.3390/ijms20153742.
14. Sun M, Voorrips RE, Vosman B. Aphid populations showing differential levels of virulence on capsicum accessions. *Insect Sci*. 2020, 27(2): 336–348. doi: 10.1111/1744-7917.12648. Epub 2018 Dec 6.
15. Leybourne DJ, Valentine TA, Robertson JAH, Pérez FE, Main AM, Karley AJ, et al. Defence gene expression and phloem quality contribute to mesophyll and phloem resistance to aphids in wild barley. *J Exp Bot*. 2019, 70(15): 4011–4026. doi: 10.1093/jxb/erz163.
16. Khan SA, Marimuthu M, Predeesh C, Aguirre RLM, Reese JC, Smith CM. Electrical penetration graph recording of russian wheat aphid (Hemiptera: Aphididae) feeding on aphid-resistant wheat and

barley. *J Econ Entomol*. 2015, 108(5): 2465–70. doi: 10.1093/jee/tov183.

17. Smith CM, Chuang WP. Plant resistance to aphid feeding: behavioral, physiological, genetic and molecular cues regulate aphid host selection and feeding. *Pest Manag Sci*. 2014, 70(4): 528–40. doi: 10.1002/ps.3689.
18. Broekgaarden C, Snoeren TA, Dicke M, Vosman B. Exploiting natural variation to identify insect-resistance genes. *Plant Biotechnol J*. 2011, 9(8): 819 – 25. doi: 10.1111/j.1467-7652.2011.00635. x.
19. Chen J, Ullah H, Tu X, Zhang Z. Understanding the genetic mechanism of resistance in aphid-treated alfalfa (*Medicago sativa* L.) through proteomic analysis. *3 Biotech*. 2019, 9(6): 241. doi: 10.1007/s13205-019-1755-z.
20. Züst T, Agrawal AA. Mechanisms and evolution of plant resistance to aphids. *Nat Plants*. 2016, 2: 15206. doi: 10.1038/nplants.2015.206.
21. Ohashi T, Miyazawa Y, Ishizaki S, Kurobayashi Y, SaitoT. Identification of odor-active trace compounds in blooming flower of damask rose (*Rosa damascena*). *J Agric Food Chem*. 2019, 67(26): 7410–7415. doi: 10.1021/acs.jafc.9b03391.
22. Soufflet FV, Araou E, Jeauffre J, Thouroude T, Chastellier A, Michel G, et al. Diversity and selection of the continuous-flowering gene, RoKSN, in rose. *Hortic Res*. 2021, 8(1): 76. doi: 10.1038/s41438-021-00512-3.
23. Huang P, Lin F, Li B, Zheng Y. Hybrid-Transcriptome sequencing and associated metabolite analysis reveal putative genes involved in flower color difference in rose mutants. *Plants (Basel)*. 2019, 8(8): 267. doi: 10.3390/plants8080267.
24. Yang FZ, Yang B, Li BB, Xiao C. Alternaria toxin-induced resistance in rose plants against rose aphid (*Macrosiphum rosivorum*): effect of tenuazonic acid. *J Zhejiang Univ Sci B*. 2015, 16(4): 264–74. doi: 10.1631/jzus. B1400151.
25. Zhu ZJ, Schultz AW, Wang JH, Johnson CH, Yannone SM, Patti GJ, et al. Liquid chromatography quadrupole time-of-flight mass spectrometry characterization of metabolites guided by the METLIN database. *Nature protocols*. 2013, 8(3): 451–460. doi: 10.1038/nprot.2013.004.
26. Xia XL, Shao YF, Jiang JF, Ren LP, Chen FD, Fang WM, et al. Gene expression profiles responses to aphid feeding in chrysanthemum (*Chrysanthemum morifolium*). *BMC Genomics.* 2014, 15(1): 1050. doi: 10.1186/1471-2164-15-1050.
27. Foyer CH, Rasool B, Davey JW, Hancock RD. Cross-tolerance to biotic and abiotic stresses in plants: a focus on resistance to aphid infestation. *J Exp Bot*. 2016, 67(7): 2025–37. doi: 10.1093/jxb/erw079.
28. Liu JF, Wang ZY, Zhao J, Zhao L, Wang L, Su Z, et al. *HrCYP90B1* modulating brassinosteroid biosynthesis in sea buckthorn (*Hippophae rhamnoides* L.) against fruit fly (*Rhagoletis batava obseuriosa* Kol.) infection. Tree Physiol. 2021, 41(3):444–459. doi: 10.1093/treephys/tpaa164.
29. Liao K, Peng YJ, Yuan LB, Dai YS, Chen QF, Yu LJ, et al. Brassinosteroids Antagonize Jasmonate-Activated Plant Defense Responses through BRI1-EMS-SUPPRESSOR1 (BES1). Plant Physiol. 2020, 182(2):1066–1082. doi: 10.1104/pp.19.01220.

30. Pan G, Liu YQ, Ji L, Zhang X, He J, Huang J, et al. Brassinosteroids mediate susceptibility to brown planthopper by integrating with the salicylic acid and jasmonic acid pathways in rice. J Exp Bot. 2018, 69(18):4433–4442. doi: 10.1093/jxb/ery223.
31. Tsuda K, Somssich IE. Transcriptional networks in plant immunity. *New Phytol*. 2015, 206(3): 932–947. doi: 10.1111/nph.13286.
32. Amorim LLB, Da FDSR, Neto JPB, Guida SM, Crovella S, Benko IAM. Transcription Factors Involved in Plant Resistance to Pathogens. *Curr Protein Pept Sci*. 2017, 18(4): 335–351. doi: 10.2174/1389203717666160619185308.
33. Li PL, Song AP, Gao CY, Jiang JF, Chen SM, Fang WM, et al. The over-expression of a chrysanthemum WRKY transcription factor enhances aphid resistance. *Plant Physiol Biochem*. 2015, 95: 26–34. doi: 10.1016/j.plaphy.2015.07.002.
34. Zhu L, Guo J, Ma Z, Wang J, Zhou C. Arabidopsis transcription factor MYB102 increases plant susceptibility to aphids by substantial activation of Ethylene biosynthesis. *Biomolecules*. 2018, 8(2): 39. doi: 10.3390/biom8020039.
35. Wang Q, Eneji AE, Kong X, Wang K, Dong H. Salt stress effects on secondary metabolites of cotton in relation to gene expression responsible for aphid development. *PLoS One*. 2015, 10(6): e0129541. doi: 10.1371/journal.pone.0129541.
36. Züst T, Agrawal AA. Mechanisms and evolution of plant resistance to aphids. *Nat Plants*. 2016, 2: 15206. doi: 10.1038/nplants.2015.206.
37. Yu X, Jia D, Duan P. Plasmid engineering of aphid alarm pheromone in tobacco seedlings affects the preference of aphids. *Plant Signal Behav*. 2019, 14(5): e1588669. doi: 10.1080/15592324.2019.1588669.
38. Kariyat RR, Gaffoor I, Sattar S, Dixon CW, Frock N, Moen J, et al. Sorghum 3-Deoxyanthocyanidin flavonoids confer resistance against corn leaf aphid. *J Chem Ecol*. 2019, 45(5–6): 502–514. doi: 10.1007/s10886-019-01062-8.
39. Enders LS, Rault LC, Heng MTM, Siegfried BD, Miller NJ. Transcriptional responses of soybean aphids to sublethal insecticide exposure. *Insect Biochem Mol Biol*. 2020, 118: 103285. doi: 10.1016/j.ibmb.2019.103285.
40. Singh V, Shah J. Tomato responds to green peach aphid infestation with the activation of trehalose metabolism and starch accumulation. *Plant Signal Behav*. 2012, 7(6): 605–7. doi: 10.4161/psb.20066.
41. Claros CJL, Pinillos EO, Tito R, Mirones CS, Gamarra MNN. Insecticidal properties of capsaicinoids and glucosinolates extracted from *Capsicum chinense* and *Tropaeolum tuberosum*. *Insects*. 2019, 10(5): 132. doi: 10.3390/insects10050132.
42. Lei J, Jayaprakash GK, Singh J, Uckoo R, Borrego EJ, Finlayson S, et al. CIRCADIAN CLOCK-ASSOCIATED1 controls resistance to aphids by altering indole glucosinolate production. *Plant Physiol*. 2019, 181(3): 1344–1359. doi: 10.1104/pp.19.00676.

43. Łukasik I, Wołoch A, Sytykiewicz H, Sprawka I, Goławska S. Changes in the content of thiol compounds and the activity of glutathione s-transferase in maize seedlings in response to a rose-grass aphid infestation. *PLoS One*. 2019, 14(8): e0221160. doi: 10.1371/journal.pone.0221160.
44. Dampc J, Kula MM, Molon M, Durak R. Enzymatic defense response of apple aphid aphis pomi to increased temperature. *Insects.* 2020, 11(7): 436. doi: 10.3390/insects11070436.
45. Sytykiewicz H. Expression patterns of genes involved in Ascorbate-Glutathione cycle in aphid-infested maize (*Zea mays* L.) seedlings. *Int J Mol Sci*. 2016, 17(3): 268. doi: 10.3390/ijms17030268.
46. Kiani M, Szczepaniec A. Effects of sugarcane aphid herbivory on transcriptional responses of resistant and susceptible sorghum. *BMC Genomics*. 2018, 19(1): 774. doi: 10.1186/s12864-018-5095-x.
47. Chen FD, Deng YM, Chen SM, Fang WM, Guan ZY, He JP, et al. A method for artificial inoculation to identify the resistance of chrysanthemum aphid. 2009, CN101520447A.
48. Zhong SL, Joung JG, Zheng Y, Chen YR, Liu B, Shao Y, et al. High-throughput illumina strand-specific RNA sequencing library preparation. Cold Spring Harbor Protocol. 2011,2011(8):940–9. doi: 10.1101/pdb. prot5652.
49. Kim D, Langmead B, Salzberg SL. HISAT: a fast-spliced aligner with low memory requirements. Nature methods. 2015, 12(4): 357. doi: 10.1038/nmeth.3317.
50. Pertea M, Pertea GM, Antonescu CM, Chang TC, Mendell JT, Salzberg SL. StringTie enables improved reconstruction of a transcriptome from RNA-seq reads. Nature biotechnology. 2015,33(3): 290–295. doi: 10.1038/nbt.3122.
51. Pertea M, Kim D, Pertea GM, Leek JT, Salzberg, S. L. Transcript-level expression analysis of RNA-seq experiments with HISAT, StringTie and Ballgown. Nature Protocols. 2016,11(9):1650–1667. doi: 10.1038/nprot.2016.095.
52. Love MI, Huber W, Anders S. Moderated estimation of fold change and dispersion for RNA-seq data with DESeq2. Genome biology. 2014, 15(12): 550. doi: 10.1186/s13059-014-0550-8.
53. Kanehisa M, Goto S. KEGG: kyoto encyclopedia of genes and genomes. Nucleic acids research. 2000, 28(1): 27–30. doi: 10.1093/nar/28.1.27.
54. Zhang Z, Thomma BP. Virus-induced gene silencing and Agrobacterium tumefaciens-mediated transient expression in Nicotiana tabacum. Methods Molecular Biology. 2014, 1127:173–181. doi: 10.1007/978-1-62703-986-4_14.
55. Chen W, Gong L, Guo ZL, Wang WS, Zhang HY, Liu XQ, et al. A novel integrated method for large-scale detection, identification, and quantification of widely targeted metabolites: application in the study of rice metabolomics. Molecular plant. 2013, 6(6): 1769–1780. doi: 10.1093/mp/sst080.
56. Wishart DS, Jewison T, Guo AC, Wilson M, Knox C, Liu Y, et al. HMDB 3.0—the human metabolome database in 2013. Nucleic acids research. 2013, 41(D1): D801-D807. doi: 10.1093/nar/gks1065.

# Figures

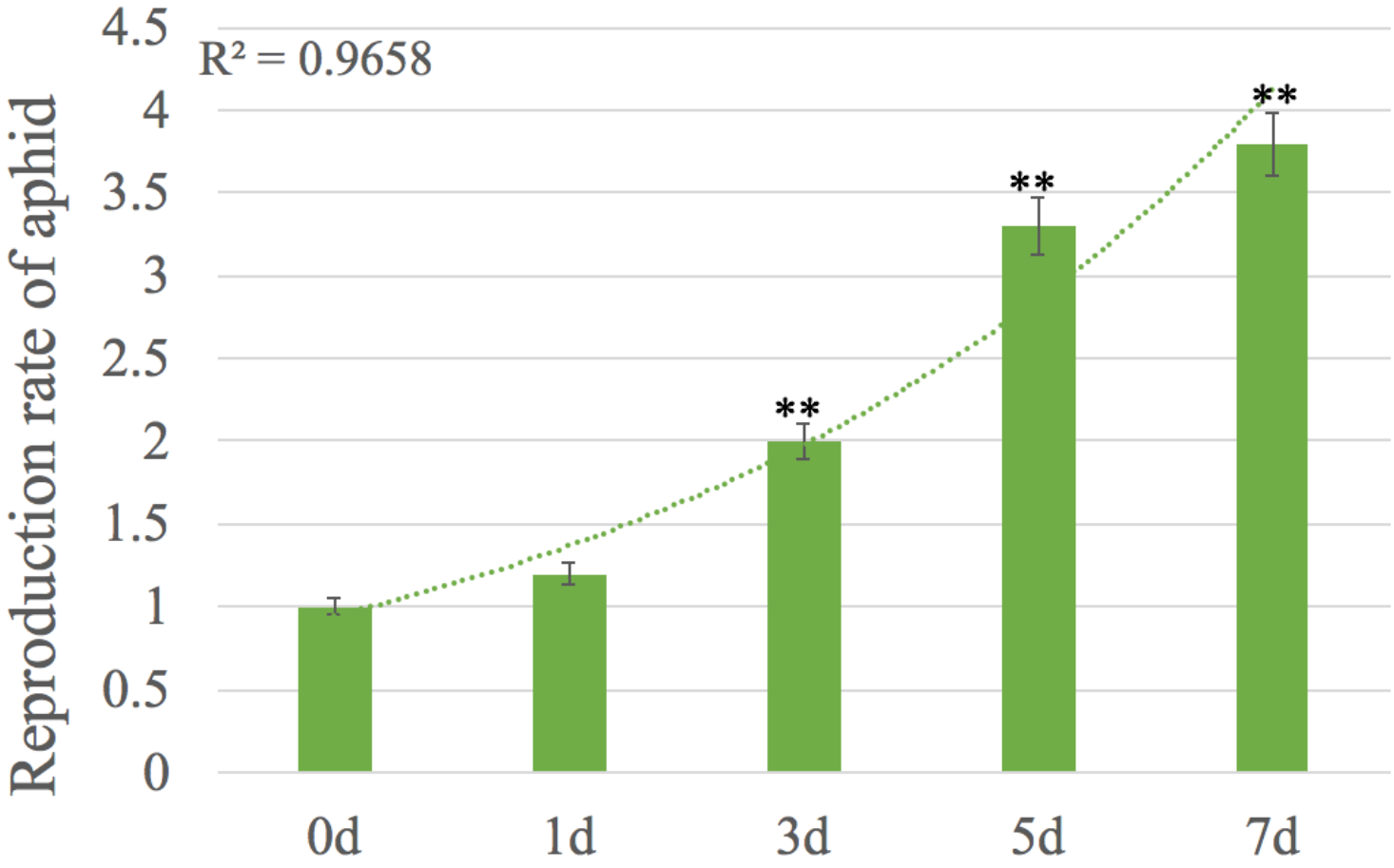


**Figure 1**

Macrosiphum rosivorum rate of reproduction of Rosa longicuspis. All statistical analyses were performed using Student's t-test; ** indicate significant differences at the P < 0.01 level.

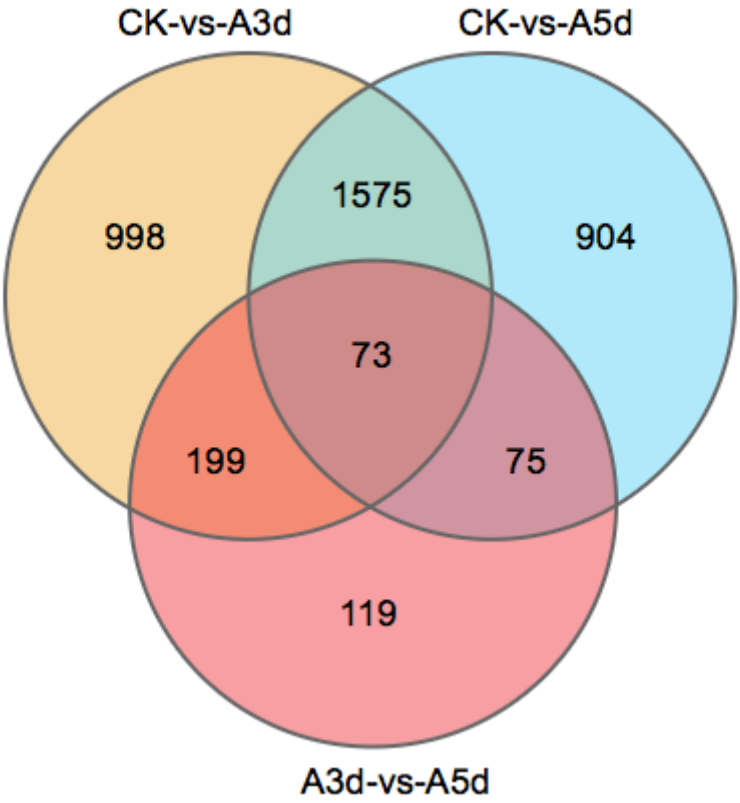


## Figure 2

Venn map of differentially expressed genes (DEGs) between CK VS A3 d, CK VS A5d and A3d VS A5 d.

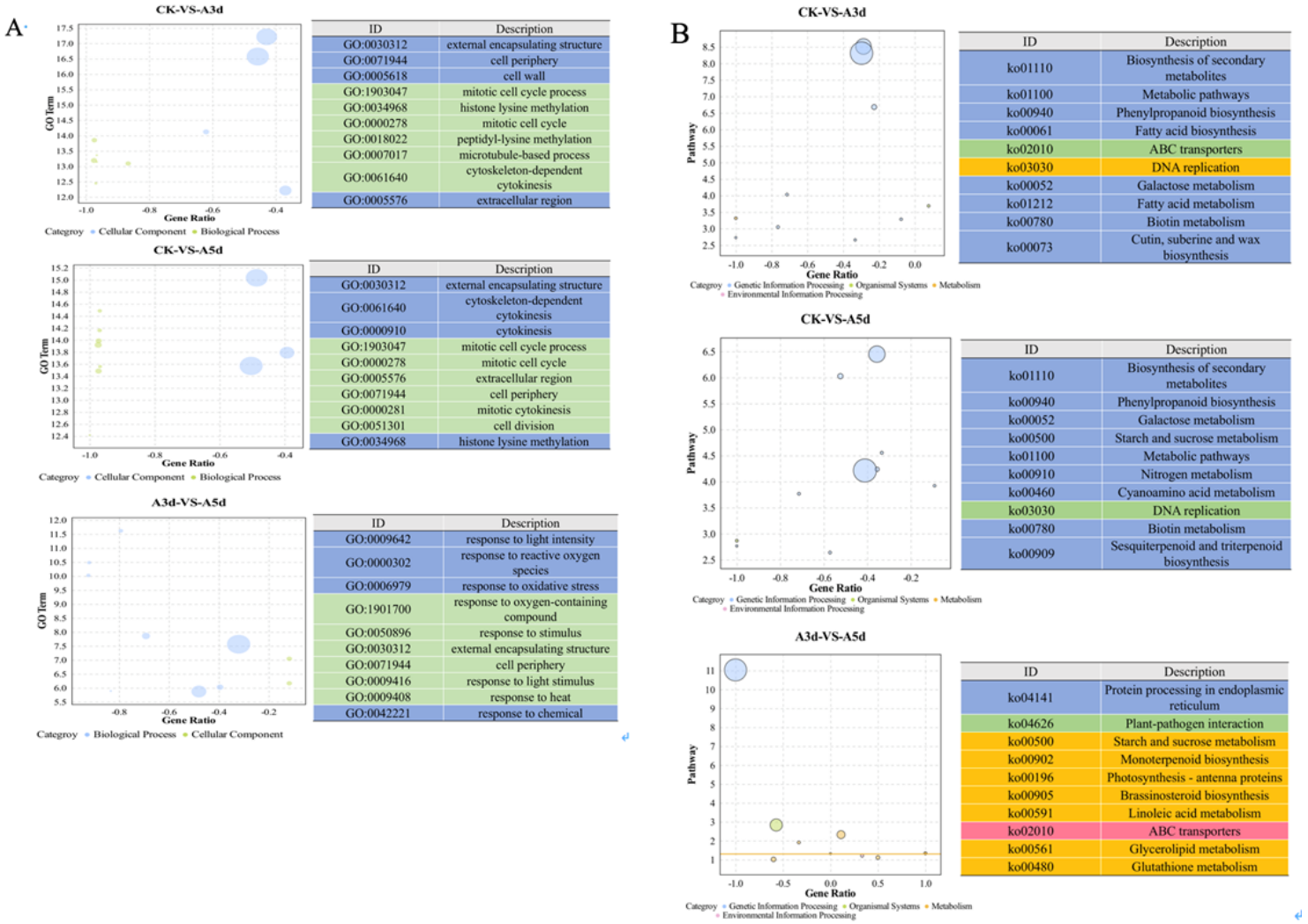


| ID | Description |
|---|---|
| GO:0030312 | external encapsulating structure |
| GO:0071944 | cell periphery |
| GO:0005618 | cell wall |
| GO:1903047 | mitotic cell cycle process |
| GO:0034968 | histone lysine methylation |
| GO:0000278 | mitotic cell cycle |
| GO:0018022 | peptidyl-lysine methylation |
| GO:0007017 | microtubule-based process |
| GO:0061640 | cytoskeleton-dependent cytokinesis |
| GO:0005576 | extracellular region |

| ID | Description |
|---|---|
| GO:0030312 | external encapsulating structure |
| GO:0061640 | cytoskeleton-dependent cytokinesis |
| GO:0000910 | cytokinesis |
| GO:1903047 | mitotic cell cycle process |
| GO:0000278 | mitotic cell cycle |
| GO:0005576 | extracellular region |
| GO:0071944 | cell periphery |
| GO:0000281 | mitotic cytokinesis |
| GO:0051301 | cell division |
| GO:0034968 | histone lysine methylation |

| ID | Description |
|---|---|
| GO:0009642 | response to light intensity |
| GO:0000302 | response to reactive oxygen species |
| GO:0006979 | response to oxidative stress |
| GO:1901700 | response to oxygen-containing compound |
| GO:0050896 | response to stimulus |
| GO:0030312 | external encapsulating structure |
| GO:0071944 | cell periphery |
| GO:0009416 | response to light stimulus |
| GO:0009408 | response to heat |
| GO:0042221 | response to chemical |

| ID | Description |
|---|---|
| ko01110 | Biosynthesis of secondary metabolites |
| ko01100 | Metabolic pathways |
| ko00940 | Phenylpropanoid biosynthesis |
| ko00061 | Fatty acid biosynthesis |
| ko02010 | ABC transporters |
| ko03030 | DNA replication |
| ko00052 | Galactose metabolism |
| ko01212 | Fatty acid metabolism |
| ko00780 | Biotin metabolism |
| ko00073 | Cutin, suberine and wax biosynthesis |

| ID | Description |
|---|---|
| ko01110 | Biosynthesis of secondary metabolites |
| ko00940 | Phenylpropanoid biosynthesis |
| ko00052 | Galactose metabolism |
| ko00500 | Starch and sucrose metabolism |
| ko01100 | Metabolic pathways |
| ko00910 | Nitrogen metabolism |
| ko00460 | Cyanoamino acid metabolism |
| ko03030 | DNA replication |
| ko00780 | Biotin metabolism |
| ko00909 | Sesquiterpenoid and triterpenoid biosynthesis |

| ID | Description |
|---|---|
| ko04141 | Protein processing in endoplasmic reticulum |
| ko04626 | Plant-pathogen interaction |
| ko00500 | Starch and sucrose metabolism |
| ko00902 | Monoterpenoid biosynthesis |
| ko00196 | Photosynthesis - antenna proteins |
| ko00905 | Brassinosteroid biosynthesis |
| ko00591 | Linoleic acid metabolism |
| ko02010 | ABC transporters |
| ko00561 | Glycerolipid metabolism |
| ko00480 | Glutathione metabolism |

## Figure 3

GO (A) and KEGG (B) analysis based on DEGs in CK VS A3 d, CK VS A5 d, and A3 d VS A5 d. (CK) non-infected rose leaves, (A3 d) Macrosiphum. rosivorum inoculated Rosa longicuspis with 3 ds, (A5 d) Macrosiphum rosivorum inoculated Rosa longicuspis with 5 ds

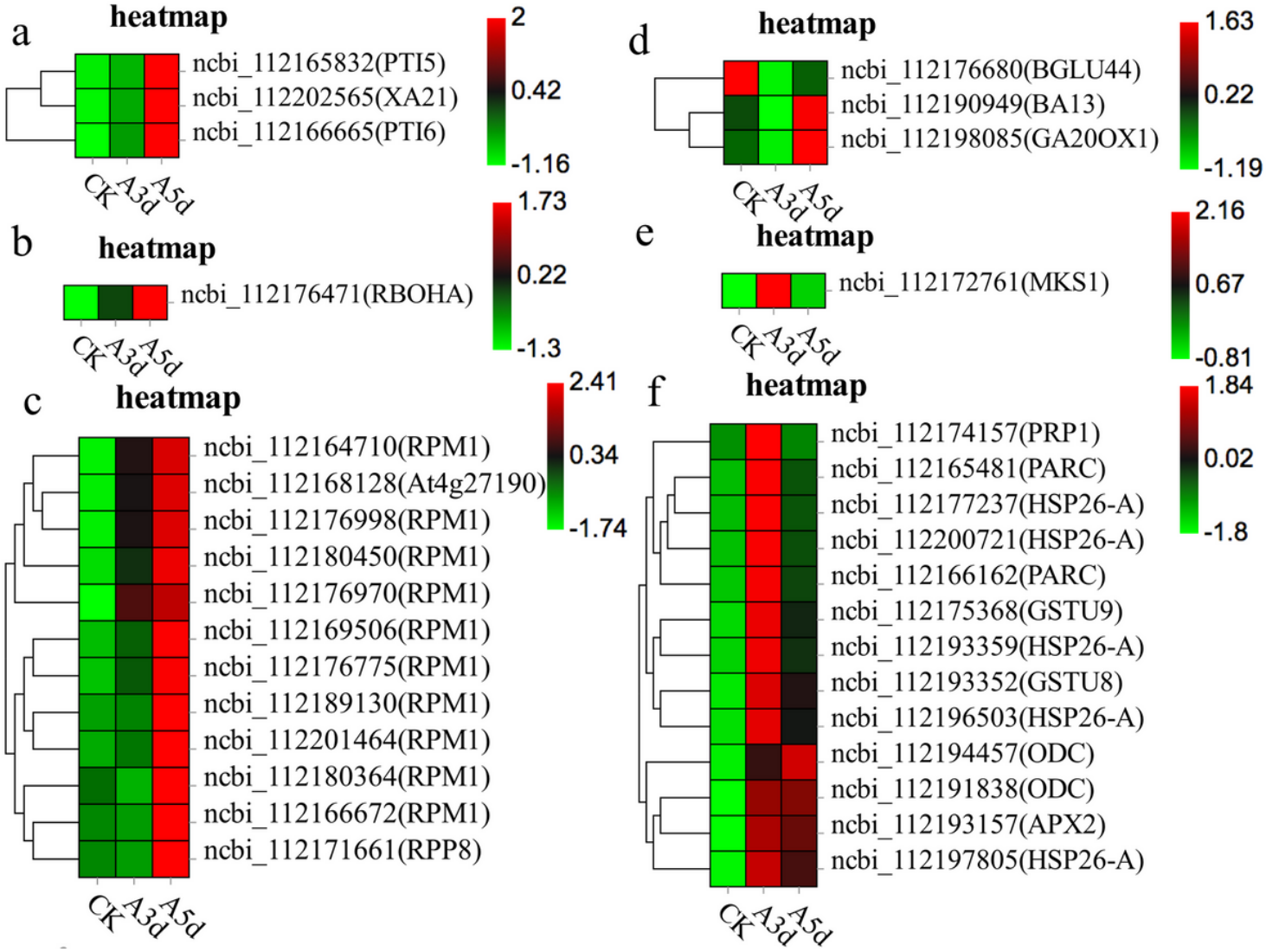


## Figure 4

Heatmap of genes in Rosa longicuspis under Macrosiphum. rosivorum stress. The bar represents the scale of the expression levels for each gene (FPKM) in the different treatments, as indicated by red/green rectangles. Genes in red show upregulation, and those in green show downregulation. (a) PTI genes, (b) ROS metabolic pathway gene, (c) Resistance protein genes, (d) Biosynthesis of secondary metabolism gene, (e) MAPK pathway gene, (c) GST genes

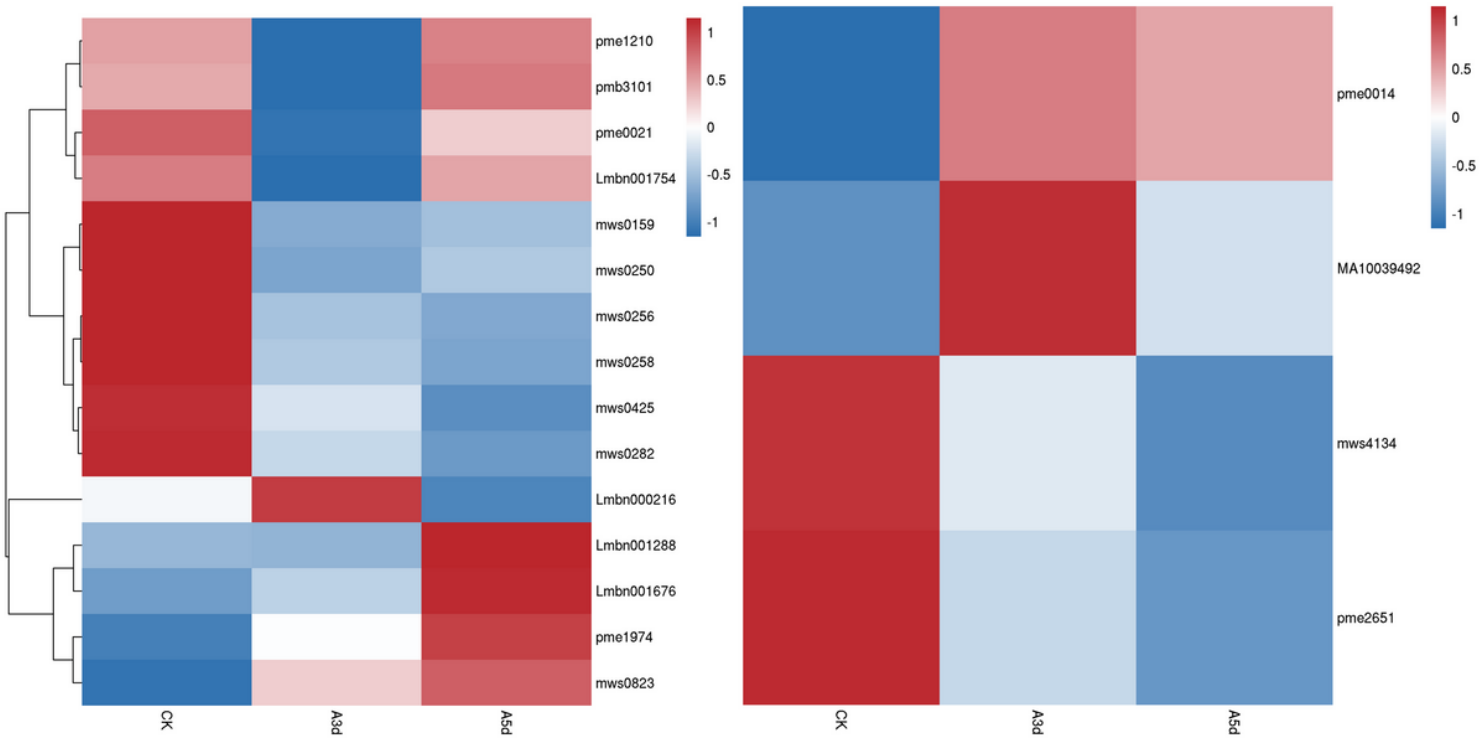


## Figure 5

Heatmap of metabolites in glucosinolate metabolism (left) and glutathione metabolism (right) pathway. The abscissa represents the sample name and hierarchical metabolite code.

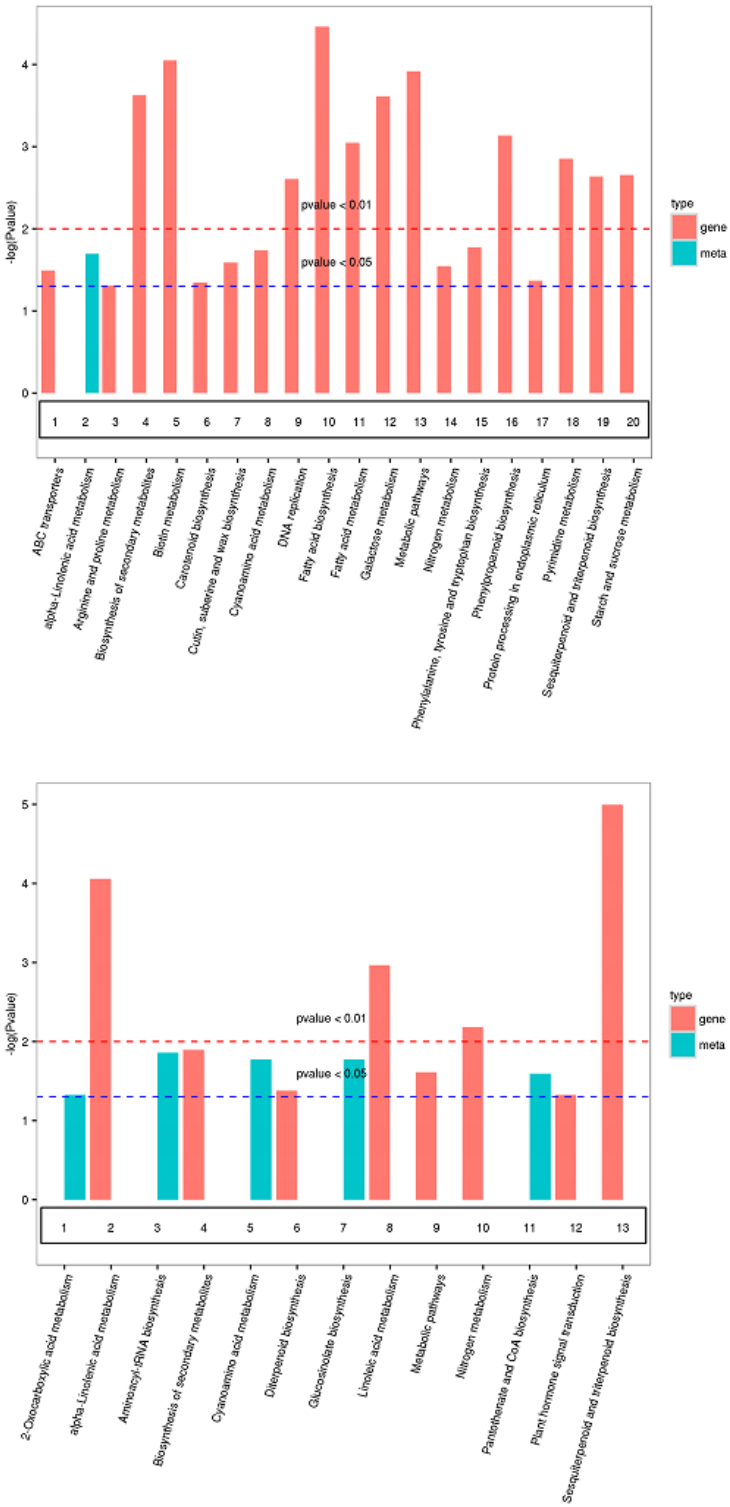


**Figure 6**

Joint KEGG enrichment p-value histogram in CK-VS-A3 d and CK-VS-A5 d.

# Supplementary Files

This is a list of supplementary files associated with this preprint. Click to download.

- supfig1all.samples.pearson.png
- figs2.pdf
- figs3.png
- figs4.png
- tables1.xlsx
- tables2.xlsx
- tables3.xls
- tables4.xls
- tables5.xls
- tables6.xls